

## Donor/Acceptor Fulleropyrrolidine Triads

M. Ángeles Herranz, Beatriz Illescas, and Nazario Martín\*

*Departamento de Química Orgánica I, Facultad de Ciencias Químicas, Universidad Complutense, E-28040 Madrid, Spain*

Chuping Luo and Dirk M. Guldi\*

*Radiation Laboratory, University of Notre Dame, Notre Dame, Indiana 46556*

*nazmar@eucmax.sim.ucm.es*

*Received April 17, 2000*

New C<sub>60</sub>-based triads, constituted by a fulleropyrrolidine moiety and two different electroactive units [donor 1-donor (**10**, **15a,b**), or donor 1-acceptor (**17**, **21**)], have been synthesized by 1,3-dipolar cycloaddition reaction of azomethyne ylides to C<sub>60</sub> and further acylation reaction on the pyrrolidine nitrogen. The electrochemical study reveals some electronic interaction between the redox-active chromophores. Triads bearing tetrathiafulvalene (TTF) and ferrocene (Fc) (**10**) or  $\pi$ -extended TTFs and Fc (**15a,b**) show reduction potentials for the C<sub>60</sub> moiety which are cathodically shifted in comparison to the parent C<sub>60</sub>. In contrast, triads endowed with Fc and anthraquinone (AQ) (**17**) or Fc and tetracyanoanthraquinodimethane (TCAQ) (**21**) present reduction potentials for the C<sub>60</sub> moiety similar to C<sub>60</sub>. Fluorescence experiments and time-resolved transient absorption spectroscopy reveal intramolecular electron transfer (ET) processes from the stronger electron donor (i.e., TTF or extended TTF) to the fullerene singlet excited state, rather than from the poorer ferrocene donor in **10**, **15a,b**. No evidence for a subsequent ET from ferrocene to TTF<sup>•+</sup> or  $\pi$ -extended TTF<sup>•+</sup> was observed.

### Introduction

The application of fullerenes as a 3-dimensional building block for the design of electroactive donor–acceptor systems emerged as a central topic in chemistry.<sup>1</sup> In these photoactive systems, a number of fullerene properties appear particularly promising to achieve efficient conversion of solar energy into useable forms of energy. For example, the low first reduction potential of [60]fullerene, comparable to those of planar quinones, and the possibility of forming stable multianions are worthy of mention.<sup>2</sup> Both of these features relate to the unique icosahedral structure of [60]fullerene and the therefrom evolving electronic configuration, namely, a small HOMO–LUMO energy gap and a maximum degeneracy of the HOMO and LUMO's.

Equally important is the low reorganization energy ( $\lambda$ ) of fullerenes in electron-transfer reactions (ET).<sup>3</sup> The Marcus ET theory treats the dependence of ET rates on the free energy changes of the reaction ( $-\Delta G$ ) as a parabolic curve.<sup>4</sup> Hereby, the forward ET lies in a region in which the rate typically increases with increasing driving force, referred to as the “normal region” of the Marcus curve ( $-\Delta G < \lambda$ ). With increasing exothermicity of the ET reaction the optimally thermodynamic conditions, that is, where the driving force equals the overall

reorganization energy ( $-\Delta G \sim \lambda$ ), are reached. Beyond this maximum the highly exergonic region ( $-\Delta G > \lambda$ ) is entered, where the rate constants actually start to decrease with increasing free energy changes (“inverted region”). Consequently, variation of  $\lambda$  is not only the key to control the maximum of the parabola, but, most importantly, to influence the shape of the parabolic dependence. In principle, smaller  $\lambda$ -values assist in reaching the maximum of the Marcus curve at smaller  $-\Delta G$  values and, in turn, in shifting the energy-wasting of back-electron transfer (BET) deep into the Marcus “inverted region”.

The covalent linkage of the electron accepting fullerenes to electron-donor fragments<sup>5,6</sup> has been thoroughly investigated in recent years with the objective to synthesize arrays that exhibit optimized ET kinetics and minimized losses of excited-state energy. Elimination of the rate-limiting diffusion between a free donor and a free acceptor moiety (i.e., not linked to each other) accelerates also the dynamics of the energy-wasting BET. In some instances, this may even lead to BET processes that are significantly faster than the forward ET (e.g., BET is around the thermodynamic maximum). In this context, the finding by Gust et al. is of particular importance, namely, that BET dynamics on the first example of a C<sub>60</sub>-based systems (**1**) are significantly slower than those of the forward ET.<sup>7</sup> This pioneering work evoked the

(1) (a) Allemand, P. M.; Koch, A.; Wudl, F.; Rubin, Y.; Diederich, F.; Alvarez, M. M.; Anz, S. J.; Whetter, R. L. *J. Am. Chem. Soc.* **1991**, *113*, 1050. (b) For a recent review, see: Echegoyen, L.; Echegoyen, L. E. *Acc. Chem. Res.* **1998**, *31*, 593.

(2) Xie, Q.; Pérez-Cordero, E.; Echegoyen, L. *J. Am. Chem. Soc.* **1992**, *114*, 3978.

(3) (a) Imahori, H.; Hagiwara, K.; Akiyama, T.; Aoki, M.; Taniguchi, S.; Okada, T.; Shirakawa, M.; Sakata, Y. *Chem. Phys. Lett.* **1996**, *263*, 545. (b) Guldi, D. M.; Asmus, K.-D. *J. Am. Chem. Soc.* **1997**, *119*, 5744.

(4) Marcus, R. A. *Angew. Chem., Int. Ed. Engl.* **1993**, *32*, 1111.

(5) Martín, N.; Sánchez, L.; Illescas, B.; Pérez, I. *Chem. Rev.* **1998**, *98*, 2527.

(6) (a) Imahori, H.; Sakata, Y. *Adv. Mater.* **1997**, *9*, 537. (b) Imahori, H.; Sakata, Y. *Eur. J. Org. Chem.* **1999**, 2445. (c) Guldi, D. M.; *Chem. Commun.* **2000**, 321.

(7) Liddell, P. A.; Sumida, J. P.; McPherson, A. N.; Noss, L.; Seely, G. R.; Clark, K. N.; Moore, A. L.; Moore, T. A.; Gust, D. *Photochem. Photobiol.* **1994**, *60*, 537.

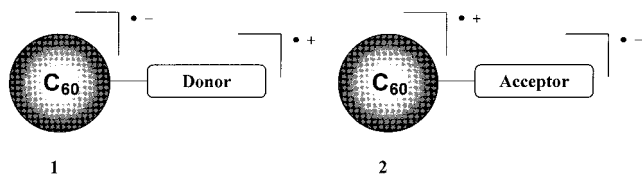


**Figure 1.** Possible ion-radicals formed from  $C_{60}$ -donor and  $C_{60}$ -acceptor dyads.

synthesis of a sheer unlimited number of  $C_{60}$ -based donor-acceptor systems incorporating a variety of electron-donor molecules<sup>5</sup> as well as photoluminescence oligomers.<sup>8</sup> Electroactive dyads of the  $C_{60}$ -acceptor type have attracted, however, lesser attention, despite their potential as multistage electron acceptors. Recent attempts to form long-lived charge-separated (CS) states (2) in  $C_{60}$ -based systems, which bear stronger acceptors than  $C_{60}$  have been mostly unsuccessful. This stems, in a first approximation, from the fact that the promotion of an electron from  $C_{60}$  to the acceptor moiety is hampered by the poor ability of fullerenes to stabilize cationic species.<sup>9</sup>

With the objective to improve the stability of the CS state in donor-acceptor arrays and, thus, to open the possibility for potential applications, two fundamentally different principles are pursued. First, the length of the intervening spacer is systematically increased. For example, a close van der Waals contact or a series of phenyl groups lead to spatial separations of  $\sim 3$  and  $18 \text{ \AA}$ , respectively. Paddon-Row et al. and also Sakata et al. reported elegant work on the synthesis of giant dyads with interchromophore separations of up to  $18 \text{ \AA}$  and CS lifetimes of  $250 \text{ ns}$ .<sup>10</sup>

The second strategy, for controlling the lifetime of the CS state, implies the incorporation of secondary and even tertiary electron donor or acceptor moieties into multi-component arrays yielding molecular triads and tetrads, respectively. In particular, designing well-defined redox gradients along multiple redox centers is the key to govern the unidirectional electron flow between various donor-acceptor couples over long distances.<sup>11</sup> In the final CS state, the charges are well-separated from each other and, in turn, BET is quite slow.

In principle three different options are feasible for the design of molecular triads, constituted by multiple electroactive units (see Figure 2). One of them is represented by the general type 3, bearing two electroactive fragments (*donor 1-donor 2* or *donor 1-acceptor*), for which representative examples have been published recently.<sup>12</sup>

Interestingly, triads of the type 4, as a meaningful alternative to 3, have not been reported so far. A probable

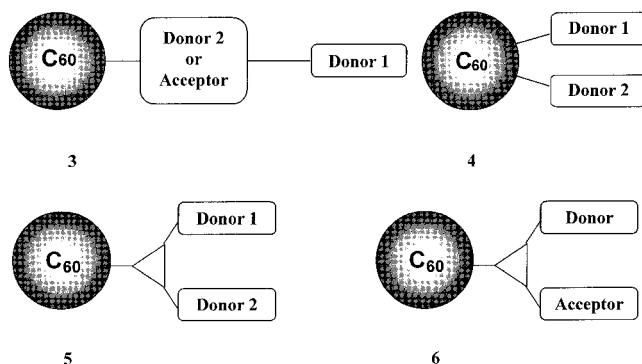


**Figure 2.** Different triads designed from  $C_{60}$ , donor, and acceptor units.

reason therefore, implies that up to nine regioisomeric bis-adducts are formed during the synthesis. The formation of isomeric mixtures renders the isolation and characterization of the formed products particularly difficult. Consequently, the development of functionalization methodologies that will provide access to multifunctional molecules, with a high control of the degree and regiochemistry of the organic addends, emerges as an important challenge in the chemistry of fullerenes.<sup>13</sup>

Nonlinear triads 5 and 6, in which all the electroactive units are linked to the same functionality (e.g., pyrrolidine ring), represent a promising alternative for the preparation of molecular triads. This type of trichromophoric systems avoids the formation of regioisomeric bis-adducts provided, however, that only a monoadduct is obtained. Triads of these types (i.e., 5 and 6) have not been reported yet and, therefore, it is of great interest to study their photophysical properties, especially under the aspect of ET reactions.<sup>14</sup>

We report in this paper on the synthesis, the electrochemical characterization and photoinduced electron-transfer studies of triads 5 and 6.  $C_{60}$  and two electron donor units of different strength constitute triads of the general type 5, while triads 6 comprise  $C_{60}$ , an electron donor and an additional electron acceptor. Ferrocene, tetrathiafulvalene (TTF) or quinonoid  $\pi$ -extended-TTF were selected as donor moieties, since they all proved to be excellent candidates for the design of the simpler  $C_{60}$ -based electroactive dyads.<sup>15,16</sup> On the other hand, 11,11,12,12-tetracyanoanthraquinodimethane (TCAQ) and its

(8) (a) Effenberger, F.; Grube, G. *Synthesis* **1998**, 1372. (b) Segura, J. L.; Martín, N. *Tetrahedron Lett.* **1999**, *40*, 3239. (c) Janssen, R. A. J.; Van Hal, P. A.; Knol, J.; Hummelen, J. K.; communication presented to the European Conference on Organic Solar Cells, ECOS, Cadarache (France), **1998**. (d) Nierengarten, J. F.; Eckert, J.-F.; Nicoud, J.-F.; Onali, L.; Krasnikov, V.; Hadziioannou, G. *Chem. Commun.* **1999**, 617. (e) Knor, S.; Grupp, A.; Mehring, M.; Grube, G.; Effenberger, F. *J. Phys. Chem.* **1999**, *110*, 3502.

(9) Martín, N.; Sánchez, L.; Illescas, B.; González, S.; Herranz, M. A.; Guldi, D. M. *Carbon* **2000**, in press, and references therein.

(10) (a) Lawson, J. M.; Oliver, A. M.; Rothenfluh, D. F.; An, Y.-Z.; Ellis, G. A.; Ranasinghe, M. G.; Khan, S. I.; Franz, A. G.; Ganapathi, P. S.; Shephard, M. J.; Paddon-Row, M. N.; Rubin, Y. *J. Org. Chem.* **1996**, *61*, 5032. (b) Williams, R. M.; Koeberg, M.; Lawson, J. M.; An, Y.-Z.; Rubin, Y.; Paddon-Row, M. N.; Verhoeven, J. W. *J. Org. Chem.* **1996**, *61*, 5055. (c) Yamada, K.; Imahori, H.; Nishimura, Y.; Yamazaki, I.; Sakata, Y. *Chem. Lett.* **1999**, 895.

(11) Jolliffe, K. A.; Langford, S. J.; Ranasinghe, M. G.; Shephard, M. J.; Paddon-Row, M. N. *J. Org. Chem.* **1999**, *64*, 1238.

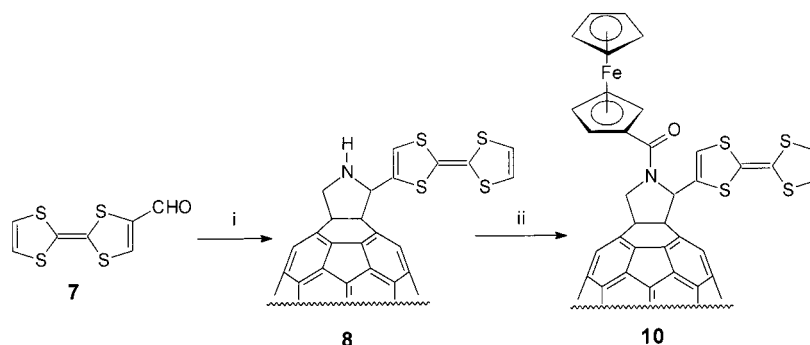
(12) (a) Liddell, P. A.; Kuciauskas, D.; Sumida, J. P.; Nash, B.; Nguyen, D.; Moore, A. L.; Moore, T. A.; Gust, D. *J. Am. Chem. Soc.* **1997**, *119*, 1400. (b) Imahori, H.; Yamada, K.; Hasegawa, M.; Taniguchi, S.; Okada, T.; Sakata, Y. *Angew. Chem., Int. Ed. Engl.* **1997**, *36*, 2626. (c) Imahori, H.; Yamada, H.; Ozawa, S.; Ushida, K.; Sakata, Y. *Chem. Commun.* **1999**, 1165. (d) Tamaki, K.; Imahori, H.; Nishimura, Y.; Yamazaki, I.; Sakata, Y. *Chem. Commun.* **1999**, 625. (e) Fujitsuka, M.; Ito, O.; Imahori, H.; Yamada, K.; Yamada, H.; Sakata, Y. *Chem. Lett.* **1999**, 721.

(13) (a) Qian, W.; Rubin, Y. *Angew. Chem., Int. Ed. Engl.* **1999**, *38*, 2356. (b) Hirsch, A. *Top. Curr. Chem.* **1999**, special issue on Fullerenes and related structures.

(14) A previous communication was presented at the Fullerenes 193rd Meeting of the Electrochemical Society, Inc.; San Diego, CA, May 3-8, 1998.

(15) (a) Guldi, D. M.; Maggini, M.; Scorrano, G.; Prato, M. *J. Am. Chem. Soc.* **1997**, *119*, 974. (b) Da Ros, T.; Prato, M.; Carano, M.; Ceroni, P.; Paolucci, F.; Roffia, S. *J. Am. Chem. Soc.* **1998**, *120*, 11645.

(16) (a) Martín, N.; Sánchez, L.; Seoane, C.; Andreu, R.; Garin, J.; Orduna, J. *Tetrahedron Lett.* **1996**, *37*, 5979. (b) Martín, N.; Pérez, I.; Sánchez, L.; Seoane, C. *J. Org. Chem.* **1997**, *62*, 5690. (c) Guldi, D. M.; González, S.; Martín, N.; Antón, A.; Garin, J.; Orduna, J. *J. Org. Chem.* **2000**, *65*, 1978. (d) Martín, N.; Sánchez, L.; Guldi, D. M. *Chem. Commun.* **2000**, 113. (e) Herranz, M. A.; Sánchez, L.; Martín, N.; Seoane, C.; Guldi, D. M. *J. Organomet. Chem.* **2000**, *599*, 2

Scheme 1<sup>a</sup>

<sup>a</sup> Reagents and conditions: (i), C<sub>60</sub>, glycine, Δ; (ii), Py, FcCOCl (9), rt.

9,10-anthraquinone (AQ) precursor were chosen as acceptor moieties, which are stronger and weaker acceptors, respectively, relative to the parent C<sub>60</sub>.<sup>17</sup>

## Results and Discussion

**Synthesis.** For the preparation of triads **10**, **15a,b**, **17**, and **21**, we selected the cycloaddition reaction of azomethine ylides to C<sub>60</sub>, following the procedure published by Prato and co-workers.<sup>18</sup> Accordingly, triad **10** was prepared in two steps starting from formyl-TTF (7). The latter is obtained via lithiation and formylation of TTF.<sup>19</sup> Reaction of formyl-TTF (7) with glycine and C<sub>60</sub> affords the TTF-containing fulleropyrrolidine (**8**)<sup>20</sup> in 30% yield (43% based on recovered C<sub>60</sub>). Despite the low basicity of fulleropyrrolidines (i.e., almost 6 orders of magnitude less basic than the parent pyrrolidine)<sup>21</sup> the amino group reacted with ferrocenecarbonyl chloride (**9**) to form triad **10** in an overall good yield (58%).

A multistep synthesis, as summarized in Scheme 2, deemed necessary for the preparation of C<sub>60</sub>-based triads of the type C<sub>60</sub>-(donor)<sub>2</sub> (**15a,b**) and C<sub>60</sub>-(donor-acceptor) (**17**, **21**). The precursor materials, namely, substituted 2-formyl-9,10-bis(1,3-dithiol-2-ylidene)-9,10-dihydroanthracenes **13a** and **13b**, were readily prepared by converting commercially available 2-hydroxymethylanthraquinone (**11**) in four steps: first, oxidation of **11** with pyridinium chlorochromate (PCC) led to **12**, to which after completing the protection of the formyl group, two dithiole rings were introduced. The final deprotection step gave then compounds **13a** and **13b**.<sup>16b</sup>

The linkage of the  $\pi$ -extended TTF molecules **13a,b** to C<sub>60</sub> required the protection of the pyrrolidine nitrogen. Thus, a reaction of *N*-tritylglycine and aldehydes **13a,b** was carried out by forming the respective azomethine ylide intermediate. These reactive intermediates react with C<sub>60</sub> to yield the *N*-trityl-protected fulleropyrrolidines **14a,b**. Deprotection of **14a,b** with trifluoromethanesulfonic acid and subsequent reaction with ferrocenecarbonyl chloride (**9**) affords products **15a** and **15b** in reasonable yields (see Scheme 2).

Triads **10** and **15a,b** were purified by chromatography and centrifugation with methanol. The structural assign-

ment of compounds **10**, **15a** and **15b** is based on analytical and spectroscopic techniques (i.e., UV-vis, FTIR, <sup>1</sup>H NMR, <sup>13</sup>C NMR and FAB mass spectra). In particular, both TTF (**10**) and  $\pi$ -extended TTF (**15a,b**) derivatives reveal in their UV-vis spectra the typical dihydrofullerene absorption band around 430 nm. The <sup>1</sup>H NMR spectrum of triad **10** shows, in addition to the signals of the ferrocene and TTF moieties (see Experimental Section), the signals of the pyrrolidine ring in form of a singlet at  $\delta$  6.80 and two doublets at  $\delta$  6.23 and  $\delta$  5.57 ( $J = 12$  Hz). On the other hand, the <sup>1</sup>H NMR spectra of compounds **15a,b** in chloroform have wider signals. Previously, this broadening has been rationalized in terms of an equilibrium between two conformations, which differ in their relative orientation of the 1,3-dithiole rings in the  $\pi$ -extended TTF moiety<sup>16b</sup> (see below).

With the objective to shed further light onto the structural identity, we recorded a <sup>13</sup>C NMR spectrum of **10**. However, the low solubility exhibited by compound **10** in organic solvents required a 3 day acquisition time in a 500 MHz apparatus. Compounds **15a,b** are more soluble and, consequently, better candidates for the <sup>13</sup>C NMR spectra. In fact, the <sup>13</sup>C NMR spectra show in addition to the amide carbonyl group at ~170 ppm, the presence of the 3 different sets of carbons (i.e., at the 6,6-ring junction, at the pyrrolidine ring and at the ferrocene moiety) in the range between 60 and 77 ppm.

The structures of the novel triads were unequivocally confirmed by mass spectroscopy using the FAB technique in positive mode (see the Experimental Section).

The precursor material for triads bearing both donor and acceptor moieties on the fulleropyrrolidine ring (**17**, **21**) is hydroxymethylanthraquinone (**11**). An outline of the synthetic concept is depicted in Scheme 2. In particular, treatment of **12** with *N*-tritylglycine and C<sub>60</sub> affords the *N*-trityl-protected dyad **16** in 30% yield (36% based on recovered C<sub>60</sub>). As a consequence of a reaction between **16** and methanesulfonic acid, the ammonium salt was collected as a precipitate. The free NH pyrrolidine was then generated upon stirring **16** with pyridine and 4-(dimethylamino)pyridine, which reacts in situ with acid chloride **9** leading to triad **17** in moderate yield.

For the preparation of 2-hydroxymethyl-TCAQ (**18**) from **11**, by using Lehnert's reagent, a 64% yield is derived.<sup>22</sup> Further oxidation of **18** with PCC afforded 2-formyl-TCAQ (**19**)<sup>17</sup> in 72% yield, which then reacted

(17) Illescas, B.; Martín, N.; Seoane, C. *Tetrahedron Lett.* **1997**, *38*, 2015.

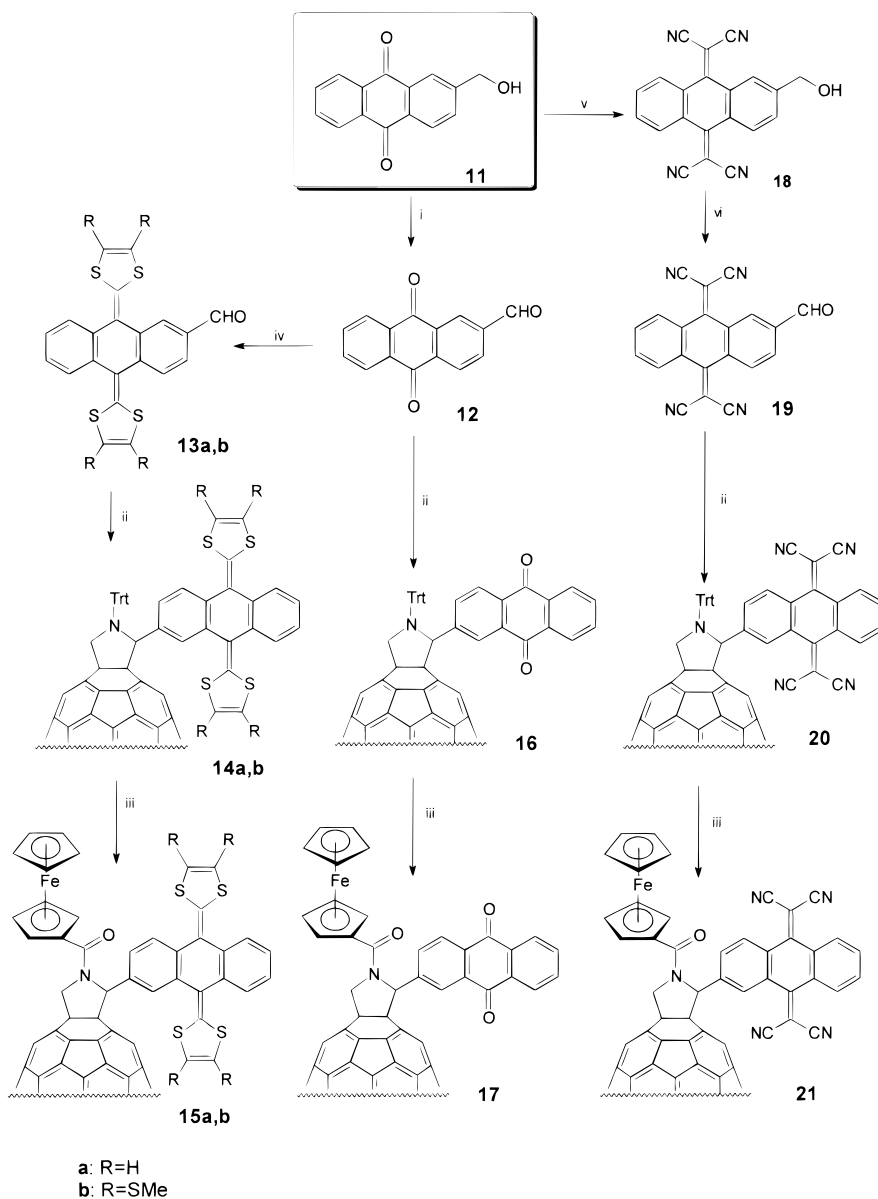
(18) Maggini, M.; Scorrano, G.; Prato, M. *J. Am. Chem. Soc.* **1993**, *115*, 9798.

(19) Garín, J.; Orduna, J.; Uriel, S.; Moore, A. J.; Bryce, M. R.; Wegener, S.; Yufit, D. S.; Howard J A K. *Synthesis* **1993**, 489.

(20) Martín, N.; Sánchez, L.; Herranz, M. A.; Guldi, D. M. *J. Phys. Chem.* **2000**, *104*, 4648.

(21) Prato, M.; Maggini, M. *Acc. Chem. Res.* **1998**, *31*, 519.

(22) (a) Lehnert, W. *Tetrahedron Lett.* **1970**, 4723. (b) Lehnert, W. *Synthesis* **1974**, 667.

Scheme 2<sup>a</sup>

<sup>a</sup> Reagents and conditions: (i) PCC, rt, CH<sub>2</sub>Cl<sub>2</sub>; (ii), C<sub>60</sub>, *N*-tritylglycine, ODCB, Δ; (iii), CF<sub>3</sub>SO<sub>3</sub>H, FcCOCl, rt, CH<sub>2</sub>Cl<sub>2</sub>; (iv) (a) HO-(CH<sub>2</sub>)<sub>3</sub>-OH, *p*-TsOH, tol., Δ, (b) phosphonate, *n*-BuLi, THF, -78 °C, (c) HCl 35%; (v), CH<sub>2</sub>(CN)<sub>2</sub>, TiCl<sub>4</sub>, py., CHCl<sub>3</sub>, Δ; Vi, PCC, rt., CH<sub>2</sub>Cl<sub>2</sub>

with *N*-tritylglycine and C<sub>60</sub> to form the corresponding *N*-trityl-protected fulleropyrrolidine (**20**) in 27% yield (47% yield based on recovered C<sub>60</sub>). Deprotection of **20** with CF<sub>3</sub>SO<sub>3</sub>H and subsequent reaction with Fc-COCl (**9**), as reported above for **16**, led to the ferrocene and TCAQ containing trichromophoric system **21** in 36% yield.

The spectroscopic data of the novel trichromophoric systems (**17**, **21**) are in agreement with the proposed structures. In particular, the <sup>1</sup>H NMR spectra of **17** and **21** show, in addition to the expected signals for the aromatic ferrocene and anthraquinone (**17**) or TCAQ (**21**) moieties, the signals of the pyrrolidine protons. These appear for **17** in form of a singlet at δ 7.46 and two doublets at δ 6.31 (*J* = 11.7 Hz) and 5.88 (*J* = 11.7 Hz).

The TCAQ fragment in **21** is known to be highly distorted, namely, an out of plane displacement caused by the strong steric repulsion between the cyano groups and the peri hydrogens.<sup>23</sup> Therefore, two different conformations are possible, depending upon the orientation

(i.e., up or down configuration of the dicyanomethylene group), similar to that noted for the donor fragment in triads **15** (see above). In fact, the <sup>1</sup>H NMR spectrum of compound **21** in chloroform at room temperature shows wide and weak signals, due to the presence of a conformational equilibrium. A much better signal resolution was found by recording the <sup>1</sup>H NMR spectrum at higher temperatures (~60 °C). This temperature accelerates the interconversion between the two isomers. Under these conditions, the signals of the pyrrolidine protons appear at δ 7.48 (s, 1H) and two doublets at δ 6.36 (*J* = 12 Hz) and 6.02 (*J* = 12 Hz).

The <sup>13</sup>C NMR spectrum of **17** shows 53 signals in the aromatic region, which indicates the lack of symmetry

(23) (a) Martín, N.; Behnish, R.; Hanack, M. J. *Org. Chem.* **1989**, *54*, 2563. (b) Bando, P.; Martín, N.; Segura, J. L.; Seoane, C. *J. Org. Chem.* **1994**, *59*, 4618. (c) Viruela, R.; Viruela, P. M.; Orti, E.; Martín, N.; *Synth. Met.* **1995**, *70*, 1031. (d) Orti, E.; Viruela, R.; Viruela, P. M. *J. Phys. Chem.* **1996**, *100*, 6138.

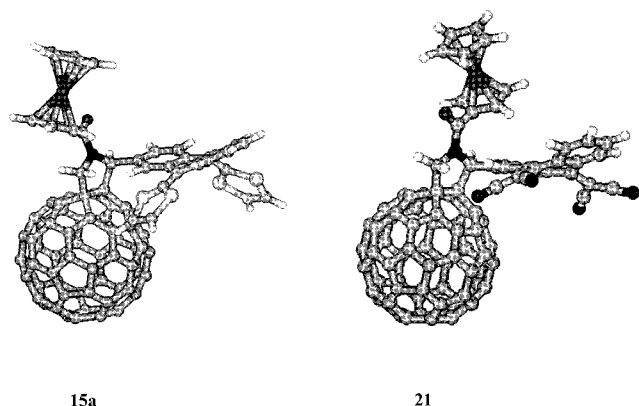


**Figure 3.** Minimum energy conformations calculated for **21** and **15a** using MM<sup>+</sup>.

in this molecule. The pyrrolidine carbons appear at  $\delta$  69.9 and 71.8 and the remaining sp<sup>3</sup> carbons of the C<sub>60</sub> core are observed at  $\delta$  75.9 and 77.2, which confirms the 6,6-junction. The analogous sp<sup>3</sup> carbons in triad **21** appear at  $\delta$  77.2 and 83.3.

The positive liquid secondary ion mass spectra (LSIMS) in a NBA matrix showed the molecular ion for **17** at *m/z* 1182 (M<sup>+</sup> + 1) and only the peak at 720 (C<sub>60</sub>, 100) was observed for **21**.

Analyzing the synthesized triads by means of X-ray crystallography was hindered by the encountered difficulties in growing defect-free single crystals. Therefore, we calculated the structure of triads **15a** and **21** by applying molecular mechanics (MM<sup>+</sup>). In principle, four conformational isomers are possible for each structure, depending upon the orientation of the 1,3-dithiole or dicyanomethylene units (i.e., up or down) and the position of the carbonyl group (i.e., inward or outward). Figure 3 represents the most stable conformation of triads **15a** and **21**, in which the 1,3-dithiole ring in **15a** and the dicyanomethylene moiety in **21** pointing downward. This conformation (**21**) is stabilized (i) by ca. 1 eV relative to that of the isomer with the dicyanomethylene pointing upward and (ii) by more than 7 eV relative to those with the ferrocene located far from the TCAQ moiety. In a similar way, the favored conformation for **15** is more than 7 eV stabilized over the other calculated structures.

**Electrochemistry.** The electrochemical behavior of the novel triads were studied by cyclic voltammetry in a toluene-acetonitrile solvent mixture (4:1 v/v) at room temperature. All the important data are collected in Table 1, along with the redox potential of [60]fullerene, TTF,  $\pi$ -extended TTF, and ferrocene as references.

Triads bearing both ferrocene and TTF (**10**) or  $\pi$ -extended TTF moieties (**15a,b**) show the presence of four reduction waves corresponding to the first four reduction steps of the fullerene moiety. All of them are cathodically shifted compared to those of the parent C<sub>60</sub>, a finding, which is reasonably well understood. In particular, saturation of a C=C double bond is responsible for raising the corresponding LUMO energy and, in turn, increasing the HOMO–LUMO gap.<sup>24</sup>

On the oxidation side, a narrow and a broad redox step were monitored for triad **10**. The first quasireversible oxidation wave, which occurs around 0.49 V, corresponds

to the formation of the radical cation of the TTF unit. The second oxidation wave follows at 0.73 V and is much broader in nature. We ascribe this process to the superimposed features of the second oxidation step of the TTF and the first oxidation step of the ferrocene unit (see Table 1).

In contrast to the two one-electron oxidation steps exhibited by TTF, only a single, but two-electron oxidation step was found for quinonoid  $\pi$ -extended TTFs.<sup>25</sup> This behavior is subject to a number of theoretical calculations at semiempirical and ab initio levels.<sup>26</sup> It should be noted that the structure of the resulting dication was confirmed in an independent study, by means of X-ray analysis.<sup>27</sup>

While triad **15a** shows two oxidation waves at 0.55 V (two electrons) and 0.75 V (one electron), only one broad oxidation wave at 0.70 V involving, however, three electrons is recorded for **15b** (Figure 4). This anodic shift reflects the substitution of the 1,3-dithiole rings. In fact, introduction of SME groups on the 1,3-dithiole ring leads to poorer electron donor systems<sup>28</sup> than the parent unsubstituted TTF (see Table 1).

The redox properties of triads **17** and **21**, which are endowed with ferrocene as a donor and either anthraquinone (**17**) or TCAQ (**21**) as an electron acceptor are also collected in Table 1 along with the parent 9,10-anthraquinone and TCAQ as internal references.

On the reduction side, triads **17** and **21** show the presence of three one-electron reduction steps, all of them taking place at the [60]fullerene moiety. Surprisingly, the reduction potential values are quite similar to those found for the parent C<sub>60</sub>. A possible reasoning for this observation stems from a combination of two effects. First, the carbonyl group linked to the pyrrolidine nitrogen decreases the reduction potential values in fulleropyrrolidines.<sup>21</sup> Second, the electronic effect of the electron-acceptor unit bound to the pyrrolidine ring shifts the reduction potential value anodically.<sup>1b,29</sup>

The reduction wave of the anthraquinone addend appears at –1.42 V for **17**. A reduction wave involving two electrons is observed at –0.34 V for **21**, corresponding to the TCAQ moiety.<sup>30</sup> (see Table 1). It is worth mentioning that the TCAQ moiety in dyad **21** gives rise to a slightly better acceptor ability than the parent unsubstituted TCAQ. This shift is probably due to the close proximity between the TCAQ and the electron-withdrawing C<sub>60</sub> core. The trichromophoric systems **17** and **21** show, in addition to the various reduction steps, an oxidation wave around +0.62 V corresponding to the formation of the radical cation of the ferrocene moiety.

(25) Yamashita, Y.; Kobayashi, Y.; Miyashi, T. *Angew. Chem., Int. Ed. Engl.* **1989**, *29*, 1450.

(26) Martín, N.; Sánchez, L.; Seoane, C.; Ortí, E.; Viruela, P. M.; Viruela, R. *J. Org. Chem.* **1998**, *63*, 1268 and references therein.

(27) Bryce, M. R.; Moore, A. J.; Hassan, M.; Ashwell, G. J.; Fraser, A. T.; Clegg, W.; Hursthouse, M. B.; Karaulov, A. I. *Angew. Chem., Int. Ed. Engl.* **1990**, *29*, 1450.

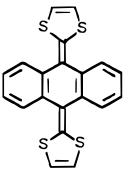
(28) Khodorkovskiy, V.; Becker, J. Y. In *Organic Conductors*; Farges, J.-P., Ed.; Marcel-Dekker: New York, 1994; Chapter 3, p 75.

(29) (a) Fernández-Paniagua, U. M.; Illescas, B.; Martín, N.; Seoane, C.; de la Cruz, P.; de la Hoz, A.; Langa, F. *J. Org. Chem.* **1997**, *62*, 3705. See also: (b) Eiermann, M.; Haddon, R. C.; Knight, B.; Li, Q. C.; Maggini, M.; Martín, N.; Ohno, T.; Prato, M.; Suzuki, T.; Wudl, F. *Angew. Chem., Int. Ed. Engl.* **1995**, *34*, 1591. (c) Knight, B.; Martín, N.; Ohno, T.; Ortí, E.; Rovira, C.; Veciana, J.; Vidal-Gancedo, J.; Viruela, P.; Viruela, R.; Wudl, F. *J. Am. Chem. Soc.* **1997**, *119*, 9871.

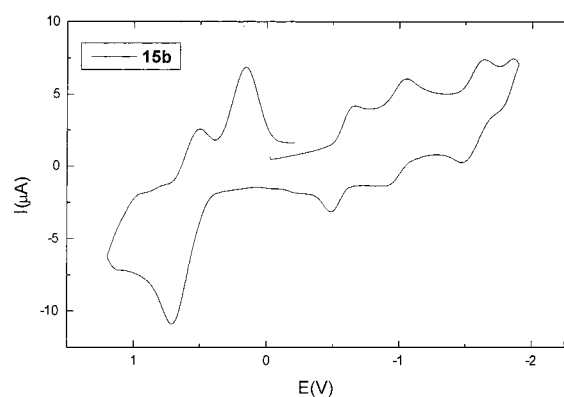
(30) (a) Aumüller, A.; Hünig, S. *Liebigs Ann. Chem.* **1984**, 618. (b) Kini, A. M.; Cowan, D. O.; Gerson, F.; Möckel, R. *J. Am. Chem. Soc.* **1985**, *107*, 556. (c) Martín, N.; Hanack, M. *J. Chem. Soc., Chem. Commun.* **1988**, 1522.

(24) Maggini, M.; Karlson, A.; Scorrano, G.; Sandona, G.; Farnia, G.; Prato, M.; *J. Chem. Soc., Chem. Commun.* **1994**, 589.

**Table 1. Redox Potentials of the C<sub>60</sub> Triads 10, 15a,b, 17, 21, and C<sub>60</sub>, Ferrocene, TTF,  $\pi$ -Extended TTF, and TCAQ as Reference Compounds**

compd	$E^1_{ox}$	$E^2_{ox}$	$E^1_{red}$	$E^2_{red}$	$E^3_{red}$	$E^A_{red}$	$E^{Org.Sust.}$
<b>10<sup>a</sup></b>	0.49	0.73 (broad)	-0.62	-1.25	-1.65	-1.96	
<b>15a<sup>a</sup></b>	0.55 (2e <sup>-</sup> )	0.75	-0.63	-1.07	-1.64	-2.14	
<b>15b<sup>a</sup></b>	0.70 (3e <sup>-</sup> ) broad		-0.66	-1.06	-1.64		
<b>17<sup>b</sup></b>	0.62		-0.59	-0.95	-1.65		-1.42
<b>21<sup>b</sup></b>	0.61		-0.60	-1.00	-1.61		-0.34 (2e <sup>-</sup> )
<b>C<sub>60</sub><sup>a</sup></b>			-0.60	-1.00	-1.52	-1.93	
<b>ferrocene<sup>a</sup></b>	0.70						
<b>TTF<sup>a</sup></b>	0.37	0.70					
	0.44 (2e <sup>-</sup> ) <sup>a</sup>						
<b>TCAQ<sup>b</sup></b>							-0.58 (2e <sup>-</sup> )

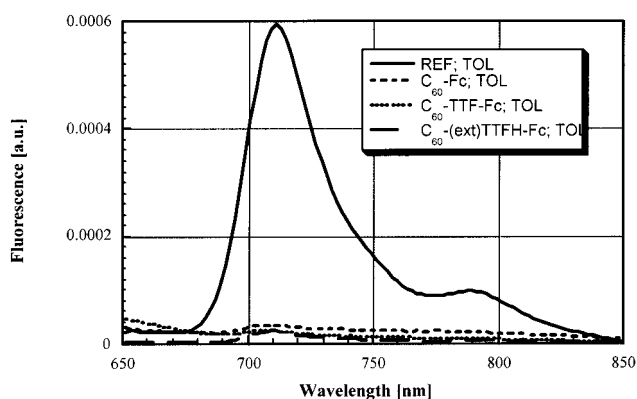
<sup>a</sup> Potentials in V vs SCE; Tol/MeCN (4:1) as solvent. <sup>b</sup> Potentials in V vs SCE; Tol/MeCN (5:1) as solvent; scan rate 200 mV/s; 0.1 mol·L<sup>-1</sup> Bu<sub>4</sub>N<sup>+</sup>ClO<sub>4</sub><sup>-</sup> as supporting electrolyte; GCE as working electrode.

**Figure 4.** Cyclic voltammogram of **15b** at 200mV/s.

In summary, the electrochemical study reveals that although the electroactive chromophores in the triads preserve their identity, a remarkable electronic interaction is observed between them.

**Photophysics.** The singlet excited-state properties of functionalized fullerene derivatives (i.e., fluorescence and singlet-singlet absorption) are sensitive measures for probing intramolecular transfer dynamics in the present donor-acceptor systems. In particular, the close spatial separation between the fullerene core and the different electron donors (i.e., ferrocene and TTF) and acceptor (i.e., TCAQ and AQ) is expected to lead to an efficient deactivation of the fullerene singlet excited state. We decided to investigate triads **10**, **15a,b**, **17**, and **21** first in a solvent of low polarity, namely, toluene and then complement these data with experiments in polar benzonitrile. In case of an intramolecular ET, using the two extreme solvents helps to vary the free energy change, associated with the ET event and, in turn, to modulate the underlying dynamics.<sup>31</sup> On the other hand, an energy transfer should be marginally, if at all, effected by the solvent polarity, since the excited state energies remain nearly constant in both solvents (see below).

A fulleropyrrolidine was selected as a reference for the steady-state and time-resolved measurements. Emission

**Figure 5.** Fluorescence spectra ( $\lambda_{exc} = 398$  nm) of *N*-methylfulleropyrrolidine, C<sub>60</sub>-Fc dyad (**23**), C<sub>60</sub>-TTF-Fc triad (**10**), and C<sub>60</sub>-extended TTF-Fc triad (**15a**) in toluene solutions at room temperature.

spectra of the fulleropyrrolidine reference in toluene and benzonitrile at room temperature show maxima around 711 nm and give rise to a moderate quantum yield of  $\sim 6.0 \times 10^{-4}$  (see Figure 5) resembling earlier reports.<sup>32</sup> Importantly, in line with the matching fluorescence quantum yields (i.e., in toluene and benzonitrile), the radiative decay of the singlet excited state ( $\tau \sim 1.5$  ns) is unchanged in these two solvents. The excitation spectrum is furthermore in excellent agreement with the UV-vis absorption features.

Corresponding experiments in a frozen matrix (at 77 K) gave furthermore evidence for a weak phosphorescence peak at 824 nm, beside a structurally well-resolved fluorescence spectrum (\*0→0, \*0→1, \*0→2 etc.). Additional evidence for the phosphorescence assignment stems from measurements, in which a heavy atom provider was added to accelerate the spin forbidden transformation from a given singlet excited state to the corresponding triplet excited state. Under these conditions, the fullerene fluorescence was completely abolished and, instead, a new band appeared at 824 nm.

Although the fluorescence pattern of the photoexcited fullerene moiety (i.e., \*0→0 emission around 711 nm) is preserved in all compounds investigated (**10**, **15a,b**, **17**,

(31) (a) Weller, A. *Z. Physik. Chem.*, **1982**, *132*, 93. (b) Gaines, G. L. I.; O'Neil, M. P.; Svec, W. A.; Niemczyk, M. P.; Wasielewski, M. R. *J. Am. Chem. Soc.*, **1991**, *113*, 719.

(32) Guldi, D. M.; Maggini, M. *Gazz. Ital. Chim.* **1998**, *127*, 779.

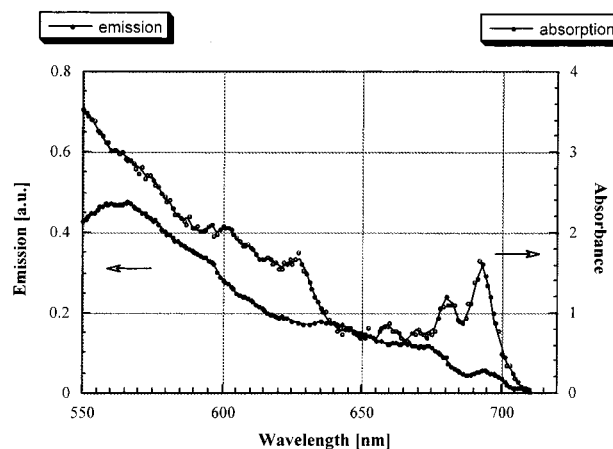
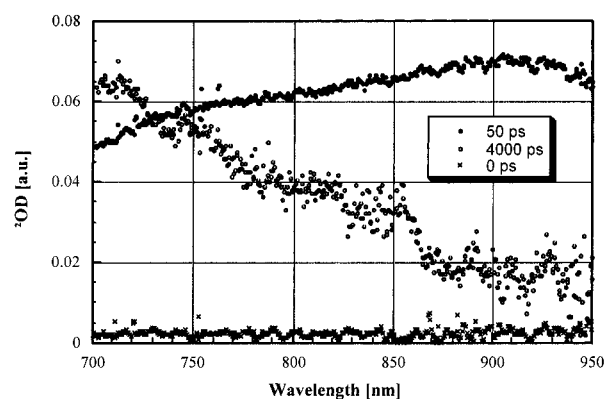
**Table 2. Fullerene Fluorescence in Nonlinear Triads 10, 15a,b, 17, and 21 and Related References (i.e., Fullero pyrrolidine and Dyads)**

compd	fluorescence quantum yield in toluene [ $\Phi \times 10^4$ ]	fluorescence quantum yield in benzonitrile [ $\Phi \times 10^4$ ]
fullero pyrrolidine	6.0	6.0
C <sub>60</sub> -Fc	0.42	0.22
<b>23</b>		
C <sub>60</sub> -TTF	0.36	0.12
C <sub>60</sub> -TTF-Fc	0.32	0.12
<b>10</b>		
C <sub>60</sub> -(extended)TTFH-Fc	0.26	<0.05
<b>15a</b>		
C <sub>60</sub> -(extended)TTFMe-Fc	0.27	0.05
<b>15b</b>		
C <sub>60</sub> -TCAQ	6.0	4.68
C <sub>60</sub> -TCAQ-Fc	0.8	0.4
<b>21</b>		
C <sub>60</sub> -AQ-Fc	0.42	0.24
<b>17</b>		

and **21**), its overall intensity (i.e., fluorescence quantum yield) is quite low, even in nonpolar toluene (see Figure 5 and Table 2). In addition, the excitation spectra of **10**, **15a,b**, **17**, and **21** in toluene bear a close resemblance with the ground-state absorption of the fullerene core (see Figure 6 for triad **21**). In general, the use of polar benzonitrile led to a further decrease of the fluorescence quantum yields. These effects stem unambiguously from (i) the short donor acceptor separation and (ii) the strongly exothermic free energy changes in both solvents. In conclusion, the steady-state fluorescence experiments reveal an efficient and, more importantly, solvent-dependent deactivation of the fullerene singlet excited state in **10**, **15a,b**, **17**, and **21**, relative to the fullero pyrrolidine reference (see above). However, at this point no meaningful assignment, from where and to where the charges transfer, can be made.

To shed further light onto the crude fluorescence quenching, triads **10**, **15a,b**, **17**, **21** were probed in time-resolved transient absorption measurements following either a 18 ps (355 nm) or a 6 ns laser pulse (337 nm). It was expected that establishing the spectral characteristics of, for example, the excited sensitizer (i.e., fullerene), oxidized donor (i.e., ferrocene, TTF, extended TTF), and reduced acceptor moieties (i.e., fullerene, TCAQ, AQ) would ease the identification of the transient intermediates and also the final photoproducts involved. Also the kinetics of the corresponding reference dyads will be employed as a valuable aid for unraveling the individual ET routes in the more complex triad structures **10**, **15a,b**, **17**, and **21**.

In particular, picosecond excitation of the fullero pyrrolidine reference led to the following characteristic absorption changes: Immediately after the laser pulse a strong absorption was monitored. A maximum around 880 nm is a clear fingerprint of the fullerene singlet-singlet absorption (Figure 7, 50 ps). The latter decays, in the 900 nm region, with a time constant of  $5.0 \times 10^8$  s<sup>-1</sup>, while a simultaneous grow-in of a new absorption dominates the absorption changes in the 700 nm region, corresponding to the fullerene triplet-triplet absorption (Figure 7, 4000 ps). The similar decay and grow-in kinetics lead to the conclusion that a spin-forbidden intersystem crossing (ISC) from the singlet excited state (1.74 eV; fluorescence at 711 nm) to the triplet excited state (1.50 eV; phosphorescence at 824 nm) takes place.

**Figure 6.** Excitation and absorption spectrum of C<sub>60</sub>-TCAQ-Fc triad (**21**) in toluene.**Figure 7.** Time-resolved difference absorption spectra of excited singlet states and excited triplet states of *N*-methylfullero pyrrolidine ( $2.0 \times 10^{-5}$  M) recorded 0, 50, and 4000 ps after excitation (355 nm) in oxygen-free toluene solution.

Further evidence for this transformation stems from the presence of an isosbestic point at around 735 nm. It should be noted that the triplet-triplet spectrum reveals another band around 380 nm (not shown).

A clean monoexponential recovery of the singlet ground state follows at low fullerene concentration and low laser power, affording a triplet lifetime of nearly 100 μs. At higher fullerene concentration and higher laser power, the kinetics become, however, more complicated. In particular, they are impacted in large by efficient (i) triplet-triplet and (ii) triplet-ground-state annihilation processes. Although substantial, these annihilation processes had, within the applied concentration range ( $\leq 5.0 \times 10^{-5}$  M), no significant impact on the fullerene singlet lifetime. In this context, the rapid singlet-singlet annihilation processes, noted in closely packed thin films of C<sub>60</sub>, as formed upon sublimation, should be mentioned.<sup>33</sup>

The initial absorption changes after the completion of the 355 nm laser pulse of **10**, **15a,b**, **17**, and **21** and the corresponding dyads are virtually superimposable to those described above for the fullero pyrrolidine reference. Again, the 880 nm maximum confirms formation of the fullerene singlet excited state. In this context it should be noted that the (extended)TTF moieties of triads **15a**

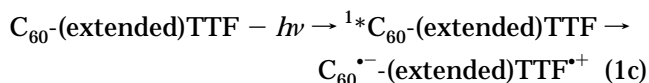
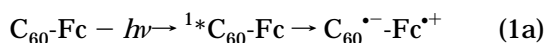
(33) Thomas, T. N.; Taylor, R. A.; Ryan, J. F.; Mihailovic, D.; Zamboni, R. In *Electronic Properties of Fullerenes*; Kuzmany, H., Fink, J., Mehring, M., Roth, S., Eds.; Springer-Verlag: Berlin, 1993; pp 292–296.

**Table 3.** Lifetime of Fullerene Singlet Excited State in Nonlinear Triads **10**, **15a,b**, **17**, and **21** and Related References (i.e., Fulleropyrrolidine and Dyads)

compd	lifetime in toluene (ps)	lifetime in benzonitrile (ps)
fulleropyrrolidine	1800	1800
<b>C<sub>60</sub>-Fc</b>	170	105
<b>23</b>		
<b>C<sub>60</sub>-TTF</b>	110	83
<b>C<sub>60</sub>-TTF-Fc</b>	107	79
<b>10</b>		
<b>C<sub>60</sub>-(extended)TTFH</b>	86	67
<b>C<sub>60</sub>-(extended)TTFH-Fc</b>	77	51
<b>15a</b>		
<b>C<sub>60</sub>-(extended)TTFsMe</b>	103	78
<b>C<sub>60</sub>-(extended)TTFsMe-Fc</b>	110	71
<b>15b</b>		
<b>C<sub>60</sub>-TCAQ</b>	1570	1340
<b>C<sub>60</sub>-TCAQ-Fc</b>	197	111
<b>21</b>		
<b>C<sub>60</sub>-AQ-Fc</b>	185	97
<b>17</b>		

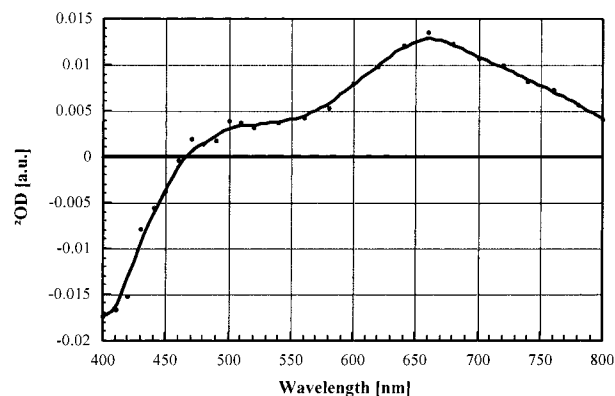
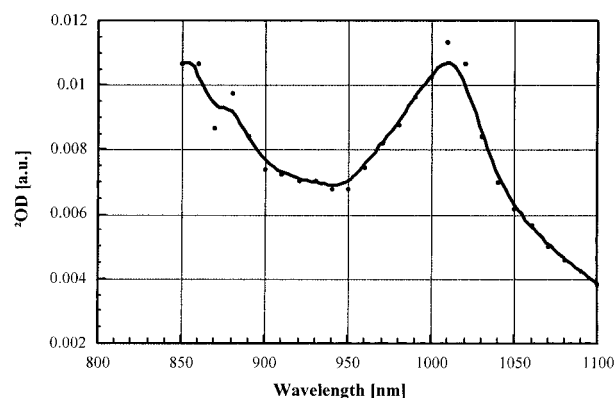
and **15b** display, in contrast to TTF or ferrocene, some absorption in the visible range.<sup>34</sup> Consequently, this observation is of particular importance, since it confirms the efficient excitation of the fullerene core. The singlet lifetimes of the fullerene moiety, which range between 51 and 110 ps (see Table 3) are, however, markedly shortened in both solvents (i.e., toluene and benzonitrile) relative to the ISC dynamics shown by the fulleropyrrolidine reference (1800 ps).

The photophysical behavior of the C<sub>60</sub>-donor dyads (Fc, TTF, (extended)TTF) has been well established and investigated in depth.<sup>15a,16c,d,20</sup> In general, the reaction scheme in these fullerene systems can be summarized as follows: Ultraviolet excitation of the respective dyad yields the fullerene singlet excited state, from which an intramolecular ET process evolves (eq 1a–c). Thereby, the only noticeable effect stems from the different oxidation strength of the donor moieties, which impacts, in turn, the underlying transfer dynamics.



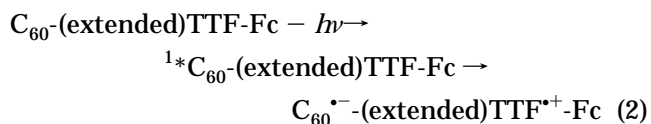
After examining the reduction potentials of the various donors in triads **10**, **15a**, and **15b** one reaches the conclusion that the TTF ( $E_{\text{ox(pa)}}^1$  (TTF/TTF<sup>•+</sup>) = 0.49 V vs SCE in **10**) and (extended)TTF ( $E_{\text{ox(pa)}}^1$  (ext.TTF/ext.TTF<sup>•+</sup>) = 0.55 vs SCE in **15a**) moieties are the primary electron donors, rather than the poorer ferrocene donor ( $E_{\text{ox(pa)}}^1$  (Fc/Fc<sup>•+</sup>) = 0.73 vs SCE in **10** and 0.75 vs SCE in **15a**) (see Table 1). Moreover, the 2  $\sigma$  bonds linking the TTF/extended TTF donors with the fullerene core versus a separation of 4  $\sigma$  bonds, in the case of the ferrocene moiety, appear to favor an ET from the TTF's.

Consequently, in both solvents the free energy changes associated with an ET between the electron accepting

**Figure 8.** Transient absorption spectrum (UV-vis part) recorded 50 ns upon flash photolysis of  $2.0 \times 10^{-5}$  M C<sub>60</sub>-extended TTF-Fc (**15a**) at 337 nm in deoxygenated benzonitrile.**Figure 9.** Transient absorption spectrum (near-IR part) recorded 50 ns upon flash photolysis of  $2.0 \times 10^{-5}$  M C<sub>60</sub>-extended TTF-Fc (**15a**) at 337 nm in deoxygenated benzonitrile.

fullerene and ferrocene donor can hardly compete with the more exothermic changes evolving from an ET between the fullerene and the various TTF donors. In fact, this consideration is further supported by the ET rates in the C<sub>60</sub>-TTF-Fc (**10**) and C<sub>60</sub>-(extended)TTF-Fc (**15a,b**) triads, which are comparable to those determined for the corresponding precursor dyads, namely, C<sub>60</sub>-TTF and C<sub>60</sub>-(extended)TTF dyads (see Table 3).

Spectral evidence for the oxidation of the (extended)-TTF rather than the ferrocene donor is also found. In particular, the transient formed upon deactivation of the fullerene singlet excited state, reveals the characteristic absorption of the (extended)TTF  $\pi$ -radical cation, absorbing at around 660 nm (Figure 8). The full characterization of the charge-separated radical pair was accomplished via detecting the fullerene  $\pi$ -radical anion through identification of its NIR fingerprint absorption<sup>35</sup> at 1000 nm (Figure 9).



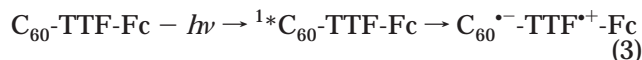
In the case of considering the ferrocene and TTF donors, no spectral comparison can be made, since none

(34) It should be noted that these donors display a minimum at the excitation wavelength, which guarantees fullerene excitation of at least 75%.

(35) Guldi, D. M.; Hungerbuehler, H.; Janata, E.; Asmus, K. D. *J. Chem. Soc., Chem. Commun* **1993**, 6, 84–86.



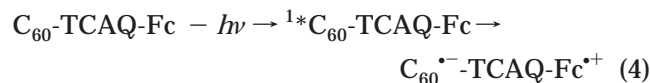
of their one-electron oxidized forms absorbs to a meaningful extent in the monitored wavelength region (i.e., 500–960 nm). In particular, the one-electron oxidized form of ferrocene shows only a very weak absorption at 625 nm ( $\epsilon = 500 \text{ L mol}^{-1} \text{ cm}^{-1}$ ),<sup>15a</sup> while the corresponding maximum of the TTF  $\pi$ -radical cation maximizes at 430 nm.<sup>20</sup> Therefore, only the ET rates allow conducting a reasonable assignment of the pathway. In line with the better electron donor properties of the TTF moiety, the dynamics suggest an intramolecular ET yielding the  $\text{C}_{60}^{\bullet-}\text{-TTF}^+\text{-Fc}$  instead of the  $\text{C}_{60}^{\bullet-}\text{-TTF-Fc}^+$  radical pair in **10**. A subsequent ET from ferrocene to  $\text{TTF}^+$  would be highly endothermic  $E_{\text{ox}}^1(\text{pa}) (\text{TTF}/\text{TTF}^+) = +0.49 \text{ V}$  versus  $E_{\text{ox}}^1(\text{pa}) (\text{Fc}/\text{Fc}^+) = +0.73 \text{ V}$ ; see Table 1), and indeed, our time-resolved experiments lacked any kinetic evidence for this unlikely reaction.



The picture is quite different in  $\text{C}_{60}\text{-AQ-Fc}$  (**17**) and  $\text{C}_{60}\text{-TCAQ-Fc}$  triads (**20**). The unfavorable free energy changes associated with an ET from the fullerene moiety to AQ or TCAQ leads to the assumption, that an exclusive reaction between the ferrocene and the fullerene moieties is expected to take place in triads **17** and **21**.<sup>36</sup>

In the case of **17** ( $\text{C}_{60}\text{-AQ-Fc}$ ), this observation is quite reasonable, since the reduction of the AQ moiety takes place at a potential, which is even passed that of the fullerene second reduction step (see Table 1). The reduction potential of TCAQ in triad **21**, on the other hand, renders to be easier than the fullerene first reduction. Nevertheless, we have recently shown that the fullerene singlet excited-state lifetime in a  $\text{C}_{60}\text{-TCAQ}$  dyad is insignificantly effected, even in polar benzonitrile and no evidence for an ET, yielding the one-electron oxidized fullerene and one-electron reduced TCAQ, namely,  $\text{C}_{60}^{\bullet+}\text{-TCAQ}^-$ , was found.<sup>9</sup>

The kinetic argument, by means of comparing the rate constants, further supports this hypothesis (see Table 3). In particular, the singlet lifetimes in the  $\text{C}_{60}\text{-AQ-Fc}$  (**17**) and  $\text{C}_{60}\text{-TCAQ-Fc}$  triads (**21**) are nearly identical with that of the  $\text{C}_{60}\text{-Fc}$  dyad. Thus, a change in direction, namely, an ET between the photoexcited fullerene and TCAQ is excluded. But, in principle, a secondary ET between the reduced fullerene ( $E_{1/2}(\text{C}_{60}/\text{C}_{60}^{\bullet-}) = -0.60 \text{ V vs SCE}$  in **21**) and TCAQ ( $E_{1/2}(\text{TCAQ}/\text{TCAQ}^-) = -0.34 \text{ V vs SCE}$  in **21**), in a thermodynamic sense, may take place. In this context, the large free energy changes for charge recombination within the  $\text{C}_{60}^{\bullet-}\text{-TCAQ-Fc}^+$  couple should, however, be compared to the small free energy changes for a subsequent ET to yield  $\text{C}_{60}\text{-TCAQ}^-\text{-Fc}^+$ . Following this argument, the second ET can be ruled out with high certainty.



The AQ moiety could serve at its best as an energy donor for an intramolecular singlet–singlet energy trans-

fer to the fullerene moiety. Similarly, we have shown in the past that the different pyrazine moieties act, in their singlet excited states as energy donors.<sup>37</sup> Since the objective of the current work is intramolecular ET reaction this possible energy transfer channel was not pursued in details and remains subject for future investigations.

**Summary and Conclusions.** In summary, we have carried out the synthesis of new types of  $\text{C}_{60}$ -based triads, formed by a fulleropyrrolidine system bearing either two electrons donor units (**10**, **15a,b**) or both electron donor and electron acceptor units (**17**, **21**) on the pyrrolidine ring. The redox properties of the triads obtained were studied by cyclic voltammetry measurements and a noticeable electronic interaction between the electroactive units was observed. Interestingly, the first reduction potential in triads bearing the anthraquinone (AQ) (**17**) or tetracyanoanthraquinodimethane (TCAQ) (**21**) acceptors are similar to that of the parent  $\text{C}_{60}$ , which has been rationalized by the combined effect of the carbonyl group on the pyrrolidine nitrogen and the electronic effect of the AQ or TCAQ acceptor on the pyrrolidine ring.

In triads **10** and **15a,b** intramolecular ET prevails from the TTF and  $\pi$ -extended TTF moieties to the fullerene singlet excited-state yielding the respective charge-separated radical pairs. An alternative ET from the ferrocene donor was not found, due to the unfavorable free energy changes associated with the ET process. In contrast, the singlet lifetimes in triads **17** and **21**, bearing the AQ and TCAQ acceptors, respectively, reveal that only a reaction between Fc as donor and  $\text{C}_{60}$  as acceptor occurs.

## Experimental Section

**General Details.**  $^1\text{H}$  NMR and  $^{13}\text{C}$  NMR spectra were obtained using a 300 and 500 MHz apparatus. Mass spectra were recorded operating at 30 kV by using a bombardment of  $\text{Cs}^+$  ions and 2-NPOE or 3-NBA as matrix. Cyclic voltammetry measurements were performed using 250 Electrochemical Analysis software. A glassy carbon electrode was used as indicator electrode in voltammetric studies ( $1 \times 10^{-5} \text{ M}$  solutions of the compound in toluene/acetonitrile (4:1 or 5:1), 0.1 M  $\text{Bu}_4\text{NClO}_4$  as the supporting electrolyte, platinum working as counter electrode and SCE as reference electrode at 20 °C).

All chromatographic experiments were performed using silica gel (70–230 mesh). All reagents were used as purchased unless otherwise stated. All solvents were dried according to standard procedures. All reactions were carried out under an atmosphere of dry argon.

Calculations were performed using molecular mechanics (MM<sup>+</sup>).

Picosecond laser flash photolysis experiments were carried out with 355-nm laser pulses from a mode-locked, Q-switched Quantel YG-501 DP (Continuum) ND:YAG laser system (pulse width (18 ps, 2–3 mJ/pulse). Passing the fundamental output through a  $\text{D}_2\text{O}/\text{H}_2\text{O}$  solution generated the white continuum picosecond probe pulse.

Nanosecond laser flash photolysis experiments were performed with laser pulses from a nitrogen laser system (337.1 nm, 8 ns pulse width, 1 mJ/pulse) in a front face excitation geometry. The photomultiplier output was digitized with a programmable digitizer.

Absorption spectra were recorded with an array spectrophotometer. Emission spectra were recorded on a Spectrofluorimeter.

(36) The lifetime of the charge-separated state in triads **10**, **15a,b**, **17**, and **21**, namely,  $\text{C}_{60}^{\bullet-}\text{-TTF}^+\text{-Fc}$ ,  $\text{C}_{60}^{\bullet-}\text{-(extended)TTF}^+\text{-Fc}$ ,  $\text{C}_{60}^{\bullet-}\text{-AQ-Fc}^+$ ,  $\text{C}_{60}^{\bullet-}\text{-TCAQ-Fc}^+$  matches those reported earlier for the corresponding dyads (see refs 15a, 16c, 16d, 20).

(37) Guldi, D. M.; Torres-Garcia, G.; Mattay, J. *J. Phys. Chem. A* **1998**, *102*, 9679.

Fluorescence spectra were measured at room temperature. A 570 nm long-pass filter in the emission path was used in order to eliminate the interference from the solvent and stray light. Long integration times (20 s) and low increments (0.1 nm) were applied. The slits were 2 and 8 nm. Each spectrum was an average of at least five individual scans.

**N-Protected Fulleropyrrolidines. General Procedure.** An *o*-dichlorobenzene (ODCB) solution (20 mL) of C<sub>60</sub> (100 mg, 0.138 mmol), the corresponding aldehyde (**7**, **12**, **13a,b**, or **19**) (0.138 mmol) and *N*-tritylglycine (207 mg, 0.69 mmol) was refluxed under argon atmosphere for a variable period of time. The solvent was removed under reduced pressure and the crude material was carefully chromatographed on silica gel column using cyclohexane/toluene, cyclohexane:ethyl acetate or cyclohexane:chloroform as eluent mixtures. Further purification was accomplished washing the solid three times with methanol.

**N-Trityl-2'-[2-[9,10-bis(1,3-dithiol-2-ylidene)anthracenyl]]pyrrolidino[3',4':1,2][60]fullerene (14a).** The reaction was refluxed under argon atmosphere during 2 h and purified using cyclohexane/toluene as eluent: 63% yield (86% based on recovered C<sub>60</sub>); <sup>1</sup>H NMR (300 MHz, CDCl<sub>3</sub>) δ 8.05 (1H, s), 7.69 (3H, m), 7.61 (3H, m), 7.10–7.45 (15H, m), 6.26 (1H, s), 6.23 (1H, s), 6.18 (1H, s), 6.16 (1H, s), 5.80 (1H, m), 5.09 (1H, m), 4.87 (1H, m); FTIR (KBr) 1570, 1541, 1507, 526 cm<sup>-1</sup>; UV-vis (CH<sub>2</sub>Cl<sub>2</sub>) λ<sub>max</sub> (log ε) 238 (5.25), 260 (5.29), 314 (4.82), 436 (4.19) nm; MS (FAB<sup>+</sup>) (*m/z*) 1142 (M<sup>+</sup> - Trt, 33%), 720 (C<sub>60</sub>, 36).

**N-Trityl-2'-[2-[9,10-bis(1,3-dithiol-4,5-methylthio-2-ylidene)anthracenyl]]pyrrolidino[3',4':1,2][60]fullerene (14b).** The reaction was refluxed under argon atmosphere during 2 h and purified using toluene as eluent: 55% yield (93% based on recovered C<sub>60</sub>); <sup>1</sup>H NMR (300 MHz, CDCl<sub>3</sub>) δ 7.97 (1H, s), 7.88 (2H, m), 7.74 (2H, m), 7.63 (2H, m), 7.25–7.54 (15H, m), 5.80 (1H, m), 5.08 (1H, m), 4.87 (1H, m), 2.37 (3H, s), 2.36 (3H, s), 2.35 (3H, s), 2.30 (3H, s); <sup>13</sup>C NMR (75 MHz, CDCl<sub>3</sub>/CS<sub>2</sub> 1:1) δ 155.9, 153.6, 147.0, 146.6, 146.0, 145.9, 145.8, 145.4, 145.3, 145.1, 144.5, 144.1, 142.8, 142.4, 142.2, 142.0, 141.5, 141.4, 140.0, 139.5, 136.1, 135.8, 135.6, 133.1, 134.3, 131.9, 127.7, 127.1, 126.8, 126.3, 125.8, 125.7, 125.3, 125.2, 125.1, 124.2, 123.3, 77.2 (C<sub>sp3</sub>-C<sub>60</sub>), 72.4 (C<sub>sp3</sub>-C<sub>60</sub>), 62.9, 61.5, 22.8, 19.7, 19.6, 19.1; FTIR (KBr) 2955, 1654, 1533, 1492, 527 cm<sup>-1</sup>; UV-vis (CH<sub>2</sub>Cl<sub>2</sub>) λ<sub>max</sub> (log ε) 227 (5.12), 256 (5.15), 308 (4.69), 439 (4.43), 632 (3.04), 701 (2.92) nm; MS (FAB<sup>+</sup>) (*m/z*) 1326 (M<sup>+</sup> - Trt, 48), 720 (C<sub>60</sub>, 100).

**N-Trityl-2'-[2-[9,10-anthraquinonyl]]pyrrolidino[3',4':1,2][60]fullerene (16).** The reaction was refluxed under argon atmosphere during 4 h and purified using a cyclohexane/ethyl acetate mixture as eluent: 30% yield (36% based on recovered C<sub>60</sub>); <sup>1</sup>H NMR (300 MHz, CDCl<sub>3</sub>) δ 8.76 (1H, s), 8.41 (1H, d, *J* = 8.1 Hz), 8.36–8.30 (3H, m), 7.81 (2H, dd, *J*<sub>1</sub> = 6.0 Hz, *J*<sub>2</sub> = 3.3 Hz), 7.33–7.13 (15H, m), 6.02 (1H, s), 5.25 (1H, d, *J* = 9.6 Hz), 5.02 (1H, d, *J* = 9.6 Hz); FTIR (KBr) 2921, 1674, 1592, 526 cm<sup>-1</sup>; UV-vis (CH<sub>2</sub>Cl<sub>2</sub>) λ<sub>max</sub> 258, 282, 314, 430, 698 nm; MS (FAB<sup>+</sup>) (*m/z*) 1219 (M<sup>+</sup> + NBA, 5), 720 (C<sub>60</sub>, 100).

**N-Trityl-2'-[2-[9,10-bis(dicyanomethylene)anthracenyl]]pyrrolidino[3',4':1,2][60]fullerene (20).** The reaction was refluxed under argon atmosphere during 4 h and purified using a cyclohexane/ethyl acetate mixture as eluent: 27% yield (47% based on recovered C<sub>60</sub>); <sup>1</sup>H NMR (300 MHz, CDCl<sub>3</sub>, 60 °C) δ 8.88 (1H, s broad), 8.35 (1H, d, *J* = 7.8 Hz), 8.31–8.17 (3H, m), 7.75 (2H, dd, *J*<sub>1</sub> = 6.0 Hz, *J*<sub>2</sub> = 3.3 Hz), 7.47–7.10 (15H, m), 5.95 (1H, s), 5.16 (1H, d, *J* = 9.9 Hz), 4.92 (1H, d, *J* = 9.9 Hz); FTIR (KBr) 2921, 2223, 1561, 1552, 1513, 526 cm<sup>-1</sup>; UV-vis (CH<sub>2</sub>Cl<sub>2</sub>) λ<sub>max</sub> 258, 286, 314, 430, 698 nm; MS (FAB<sup>+</sup>) (*m/z*) 1315 (M<sup>+</sup> + NBA, 9), 720 (C<sub>60</sub>, 100).

**2-Methyl-3,4-fulleropyrrolidine (22).** Acetaldehyde (0.42 mmol), glycine (0.29 mmol), and fullerene (0.14 mmol) were mixed in 10 mL of ODCB. The solution was refluxed for 3 h. The solvent was removed in a vacuum and the residue chromatographed over a silica gel column using a cyclohexane/toluene mixture as eluent: 10% yield (66% based on recovered C<sub>60</sub>); <sup>1</sup>H NMR (300 MHz, CDCl<sub>3</sub>) δ 4.96 (1H, d, *J* = 12.0 Hz), 4.82 (1H, d, *J* = 6.6 Hz), 4.72 (1H, d, *J* = 12.0 Hz), 2.10 (3H, d, *J* = 6.6 Hz); <sup>13</sup>C NMR (75 MHz, CDCl<sub>3</sub>/CS<sub>2</sub> 1:1) δ 155.8,

154.1, 154.0, 152.4, 146.9, 146.3, 146.2 (2C), 146.1 (2C), 146.0, 145.9, 145.8, 145.7, 145.5, 145.3, 145.2, 145.1 (2C), 145.0 (2C), 144.4, 144.3, 144.2, 144.1, 143.1, 142.9, 142.6, 142.5, 142.4, 142.2, 142.1, 142.0, 141.9, 141.8, 141.7, 141.6, 140.2, 140.1, 140.0, 139.8, 136.5, 135.6, 135.3, 78.5 (C<sub>sp3</sub>-C<sub>60</sub>), 77.2 (C<sub>sp3</sub>-C<sub>60</sub>), 75.5, 69.7, 29.8 (CH<sub>3</sub>); FTIR (KBr) 2920, 1600, 1450, 1425, 527 cm<sup>-1</sup>; UV-vis (CH<sub>2</sub>Cl<sub>2</sub>) λ<sub>max</sub> (log ε) 276 (4.72), 312 (4.47), 434 (3.58) nm; MS (MALDI) (*m/z*) 778 (M<sup>+</sup>, 56).

**2'-(Tetrathiafulvalenyl)pyrrolidino[3',4':1,2][60]fullerene (8).** This compound has been synthesized by following the previously reported procedure.<sup>21</sup>

**N-Ferrocenecarbonyl-2'-methyl[3',4':1,2][60]fullerene (23).** A CH<sub>2</sub>Cl<sub>2</sub> suspension of the corresponding fulleropyrrolidine (**22**) (28 mg, 0.036 mmol) was treated at room temperature with pyridine (0.72 mL) and 4-(dimethylamino)pyridine (7.2 mg) followed by an excess (0.108 mmol) of ferrocenecarbonyl chloride. After 1 h at ambient temperature (TLC, CH<sub>2</sub>Cl<sub>2</sub>) the solution was concentrated in vacuo and purified by flash chromatography (eluant: toluene) yielding the expected product, further purification was accomplished by repetitive precipitation and centrifugation using methanol as solvent: 28% yield; <sup>1</sup>H NMR (300 MHz, CDCl<sub>3</sub>) δ 6.45 (1H, d, *J* = 7.0 Hz), 6.21 (1H, d, *J* = 11.5 Hz), 5.28 (1H, d, *J* = 11.5 Hz), 4.99 (2H, m), 4.53 (5H, s), 2.24 (3H, d, *J* = 7.0 Hz); <sup>13</sup>C NMR (75 MHz, CDCl<sub>3</sub>/CS<sub>2</sub> 1:1) δ 169.6 (NC=O), 155.4, 154.8, 153.1, 152.7, 151.6, 149.8, 148.5, 147.9, 147.4, 147.2, 146.4, 146.3, 146.2, 146.1, 145.7, 145.5, 145.4, 145.0, 144.7, 144.6, 144.4, 143.1, 142.7, 142.4, 142.3, 142.2, 142.1, 142.0, 141.6, 140.2, 140.1, 137.1, 136.6, 135.5, 134.8, 77.7 (C<sub>sp3</sub>-C<sub>60</sub>), 77.3 (C<sub>sp3</sub>-C<sub>60</sub>), 73.9, 71.0, 70.5 (2C), 70.4, 70.3, 70.2, 70.1, 63.5, 21.1 (CH<sub>3</sub>); FTIR (KBr) 1624, 1454, 1402, 528 cm<sup>-1</sup>; UV-vis (CH<sub>2</sub>Cl<sub>2</sub>) λ<sub>max</sub> (log ε) 276 (4.80), 314 (4.55), 434 (3.56), 490 (3.35) nm; MS (MALDI) (*m/z*) 989 (M<sup>+</sup>, 53).

**N-Ferrocenecarbonyl-2'-(tetrathiafulvalenyl)pyrrolidino[3',4':1,2][60]fullerene (10).** A CH<sub>2</sub>Cl<sub>2</sub> suspension of the corresponding fulleropyrrolidine (**8**) (20 mg, 0.021 mmol) was treated at room temperature with pyridine (0.42 mL) and 4-(dimethylamino)pyridine (4.2 mg) followed by an excess (0.063 mmol) of ferrocenecarbonyl chloride. After 1 h with stirring the solution was concentrated in vacuo and purified by flash chromatography (eluant: toluene) yielding the expected product, further purification was accomplished by repetitive precipitation and centrifugation using methanol as solvent: 58% yield; <sup>1</sup>H NMR (300 MHz, CDCl<sub>3</sub>/CS<sub>2</sub> 1:1) δ 7.21 (1H, s), 6.80 (1H, s), 6.35 (2H, s), 6.23 (1H, d, *J* = 12.0 Hz), 5.57 (1H, d, *J* = 12.0 Hz), 5.05 (2H, m), 4.55 (2H, m), 4.38 (5H, s); <sup>13</sup>C NMR (125 MHz, CDCl<sub>3</sub>/CS<sub>2</sub> 1:1) δ 169.7 (NCO), 147.4, 147.3, 146.2, 146.1, 146.0, 145.9, 145.8, 145.6, 145.5, 145.4, 145.3, 145.2 (2C), 145.1, 144.6, 144.5, 144.4, 144.3, 144.2, 143.0, 142.9, 142.6, 142.5, 142.2, 142.1, 142.0, 141.9, 141.8 (2C), 141.7, 140.4, 140.3, 140.1, 140.0, 139.8, 136.9, 133.9, 133.8, 133.5, 133.4, 132.6, 132.3, 132.0, 131.9, 131.7 (2C), 131.6 (2C), 129.9, 129.4, 128.6, 128.5, 128.4, 128.3, 128.2, 127.6, 127.1, 125.0, 124.7, 119.1, 119.0, 80.9 (C<sub>sp3</sub>-C<sub>60</sub>), 75.7 (C<sub>sp3</sub>-C<sub>60</sub>), 74.2, 71.0, 70.8, 70.4, 67.8, 64.3; FTIR (KBr) 2330, 1632, 1540, 1449, 527 cm<sup>-1</sup>; UV-vis (CH<sub>2</sub>Cl<sub>2</sub>) λ<sub>max</sub> (log ε) 232 (4.85), 258 (4.96), 314 (4.62), 430 (4.04) nm; MS (FAB<sup>+</sup>) (*m/z*) 1177 (M<sup>+</sup>, 18), 720 (C<sub>60</sub>, 30).

**Triads from N-Protected Fulleropyrrolidines. General Procedure.** To a suspension of the corresponding protected fulleropyrrolidine (**14a,b**, **16**, or **20**) in 5 mL of methylene dichloride, 0.05 mL of trifluoromethanesulfonic acid was added and the mixture was stirred at room temperature for 1 h. The resulting precipitate was centrifuged, washed several times with diethyl ether and then dried under reduced pressure. This solid was later suspended in methylene dichloride (5 mL) and treated at room temperature with pyridine (0.3 mL) and 4-(dimethylamino)pyridine (3 mg) followed by an excess (3 equiv) of ferrocenecarbonyl chloride. After 1 h at ambient temperature (TLC, toluene) the clear solution was concentrated in vacuo and purified by flash chromatography (eluant: toluene, toluene/ethyl acetate or methylene dichloride). Further purification was accomplished by repetitive precipitation and centrifugation using methanol as solvent.

**N-Ferrocenecarbonyl-2'-[2-[9,10-bis(1,3-dithiol-2-ylidene)anthracenyl]]pyrrolidino[3',4':1,2][60]fullerene (15a).** The product was purified using toluene as eluent: 39% yield;  $^1\text{H NMR}$  (300 MHz,  $\text{CDCl}_3$ )  $\delta$  8.15 (1H, s), 7.79 (4H, m), 7.37 (2H, m), 6.32 (4H, m), 5.81 (1H, m), 5.00 (1H, m), 4.83 (1H, m), 4.45 (2H, m), 4.42 (2H, m), 4.27 (5H, m);  $^{13}\text{C NMR}$  (75 MHz,  $\text{CDCl}_3/\text{CS}_2$  1:2)  $\delta$  170.0 (NCO), 150.3, 147.7, 147.4, 146.2, 146.1, 146.0, 145.4, 145.3, 144.4, 143.1, 142.6, 142.5, 142.1, 142.0, 141.9, 140.3, 137.6, 137.1, 135.2, 126.5, 126.2, 126.1, 125.1, 121.9, 117.8, 117.3, 117.2, 116.8, 77.2 ( $\text{C}_{\text{sp}^3}-\text{C}_{60}$ ), 76.0 ( $\text{C}_{\text{sp}^3}-\text{C}_{60}$ ), 74.1, 72.6, 72.1, 71.8, 71.6, 70.8, 70.7, 70.2, 67.8, 63.1; FTIR (KBr) 2922, 1629, 1544, 1508, 1451, 527  $\text{cm}^{-1}$ ; UV-vis ( $\text{CH}_2\text{Cl}_2$ )  $\lambda_{\text{max}}$  ( $\log \epsilon$ ) 227 (5.13), 244 (5.13), 255 (5.14), 312 (4.68), 365 (4.42), 431 (4.39) nm; MS (FAB $^+$ ) ( $m/z$ ) 1345 ( $\text{M}^+$ , 26), 720 ( $\text{C}_{60}$ , 100).

**N-Ferrocenecarbonyl-2'-[2-[9,10-bis(1,3-dithiol-4,5-methylthio-2-ylidene)anthracenyl]]pyrrolidino[3',4':1,2][60]fullerene (15b).** The product was purified using toluene as eluent: 41% yield;  $^1\text{H NMR}$  (300 MHz,  $\text{CDCl}_3$ )  $\delta$  8.00 (1H, s), 7.77 (1H, m), 7.62 (3H, m), 7.46–7.33 (2H, m), 5.91 (1H, m), 5.03 (1H, m), 4.92 (1H, m), 4.47(3H, m), 4.31 (3H, m), 4.25 (3H, m), 2.43–2.18 (12H, m);  $^{13}\text{C NMR}$  (75 MHz,  $\text{CDCl}_3/\text{CS}_2$  1:1)  $\delta$  169.9 (NCO), 155.5, 151.7, 147.4, 147.3, 147.2, 146.2, 146.1, 146.0, 145.6, 145.5, 145.4, 145.3, 145.2, 145.1, 144.5, 144.4, 144.3, 144.2, 143.1, 142.9, 142.6, 142.3, 142.2, 142.1, 141.9, 141.8, 141.7, 140.3, 140.0, 138.3, 137.9, 136.5, 136.4, 135.6, 135.3, 134.7, 134.4, 134.3, 134.2, 129.2, 127.7, 126.7, 126.5, 126.4, 126.3, 126.0, 125.5, 125.3, 124.8, 124.0, 123.8, 123.3, 122.1, 77.2 ( $\text{C}_{\text{sp}^3}-\text{C}_{60}$ ), 75.7 ( $\text{C}_{\text{sp}^3}-\text{C}_{60}$ ), 72.1, 71.8, 71.1, 71.0, 70.9, 70.8, 70.7, 70.0, 69.1, 65.8, 60.5, 19.7, 19.5, 19.2, 19.1; FTIR (KBr) 2916, 1629, 1533, 1494, 1451, 526  $\text{cm}^{-1}$ ; UV-Vis ( $\text{CH}_2\text{Cl}_2$ )  $\lambda_{\text{max}}$  ( $\log \epsilon$ ) 227 (5.04), 247 (5.06), 255 (5.07), 312 (4.57), 442 (4.30), 699 (2.28) nm; MS (FAB $^+$ ) ( $m/z$ ) 1538 ( $\text{M}^+$ , 16), 720 ( $\text{C}_{60}$ , 34).

**N-Ferrocenecarbonyl-2'-[2-[9,10-anthraquinonyl]]pyrrolidino[3',4':1,2][60]fullerene (17).** The product was purified using toluene/ethyl acetate as eluent: 36% yield;  $^1\text{H NMR}$  (300 MHz,  $\text{CDCl}_3$ )  $\delta$  8.86 (1H, s), 8.46 (1H, d,  $J = 7.8$  Hz), 8.38–8.27 (3H, m), 7.82–7.70 (2H, m), 7.46 (1H, s), 6.31 (1H, d,  $J = 11.7$  Hz), 5.88 (1H, d,  $J = 11.7$  Hz), 5.06–4.90 (3H, m),

4.55 (1H, m), 4.35 (5H, m);  $^{13}\text{C NMR}$  (75 MHz,  $\text{CDCl}_3/\text{CS}_2$  1:1)  $\delta$  182.9 (CO), 182.6 (CO), 171.3 (NCO), 154.9, 153.7, 153.1, 151.2, 147.5, 147.4, 146.7, 146.4, 146.3 (2C), 146.1, 145.6, 145.5, 145.4, 145.3, 144.9, 144.7, 144.6 (2C), 144.5, 144.3, 144.2, 143.2, 143.1, 142.7, 142.3, 142.1, 142.0, 141.9, 141.8, 140.4, 140.3, 139.8, 136.8, 136.0, 135.4, 134.8, 134.4, 134.2, 134.1, 134.0, 133.6, 133.5, 133.3, 133.2, 130.5, 129.0, 128.3, 128.2, 127.7, 127.3, 125.4, 125.2, 77.2 ( $\text{C}_{\text{sp}^3}-\text{C}_{60}$ ), 75.9 ( $\text{C}_{\text{sp}^3}-\text{C}_{60}$ ), 72.7, 72.2, 71.8, 71.1, 70.9, 70.8, 70.3, 70.2, 69.9; FTIR (KBr) 2921, 1766, 1713, 1673, 526,  $\text{cm}^{-1}$ ; UV-vis ( $\text{CH}_2\text{Cl}_2$ )  $\lambda_{\text{max}}$  256, 280, 316, 429, 697, nm; MS (FAB $^+$ ) ( $m/z$ ) 1182 ( $\text{M}^+ + 1$ , 94), 720 ( $\text{C}_{60}$ , 100).

**N-Ferrocenecarbonyl-2'-[2-[9,10-bis(dicyanomethylene)anthracenyl]]pyrrolidino [3',4':1,2][60]fullerene (21).** The product was purified using toluene/ethyl acetate as eluent: 31% yield;  $^1\text{H NMR}$  (300 MHz,  $\text{CDCl}_3$ )  $\delta$  8.76 (1H, s), 8.36 (1H, d,  $J = 8.4$  Hz), 8.29–8.23 (3H, m), 7.77–7.74 (2H, m), 7.35 (1H, s), 7.48 (1H, s), 6.36 (1H, d,  $J = 12.0$  Hz), 6.01 (1H, d,  $J = 12.0$  Hz), 5.09–5.05 (2H, m), 4.60 (2H, m), 4.35 (4H, s);  $^{13}\text{C NMR}$  (75 MHz,  $\text{CDCl}_3/\text{CS}_2$  1:1)  $\delta$  172.7 (NCO), 159.5, 147.5, 147.4, 147.0, 146.4, 146.3, 146.2, 145.6, 145.5 (2C), 145.4, 145.3 (2C), 144.8, 144.7, 144.5, 144.4, 144.3, 143.2, 143.1, 142.2, 142.1, 142.0 (2C), 141.9, 141.8, 140.5, 140.3, 139.9, 139.3, 138.4, 132.7, 132.6, 130.9, 130.1, 130.0 (2C), 129.1, 128.8, 128.7, 128.4, 127.7, 124.4, 123.9, 119.1, 112.9, (2 x C(N), 83.3 ( $\text{C}_{\text{sp}^3}-\text{C}_{60}$ ), 77.2 ( $\text{C}_{\text{sp}^3}-\text{C}_{60}$ ), 72.1, 72.0, 71.8, 71.6, 71.3, 70.4, 70.3, 70.2; FTIR (KBr) 2922, 2223, 1449, 527  $\text{cm}^{-1}$ ; UV-vis ( $\text{CH}_2\text{Cl}_2$ )  $\lambda_{\text{max}}$  258, 290, 294, 314, 430, 696 nm; MS (FAB $^+$ ) ( $m/z$ ) 720 ( $\text{C}_{60}$ , 100).

**Acknowledgment.** Support of this work by the DGESIC of Spain (PB98-0818) is gratefully acknowledged. Some of this work was supported by the Office of Basic Energy Sciences of the U.S. Department of Energy (contribution No. NDRL-4249 from the Notre Dame Radiation Laboratory). M.A.H. is indebted to MEC for a research fellowship.

JO0005767